Revisiting Scaling Laws for Robotic Mobility in Granular Media

Article *in* IEEE Robotics and Automation Letters · January 2020

DOI: 10.1109/LRA.2020.2968031

6 authors, including:

Andrew Thoesen
Arizona State University
7 PUBLICATIONS **49** CITATIONS

SEE PROFILE

Teresa Mcbryan
Arizona State University
3 PUBLICATIONS **2** CITATIONS

SEE PROFILE

Revisiting Scaling Laws for Robotic Mobility in Granular Media

Andrew Thoesen, Teresa McBryan, Marko Green, Darwin Mick, Justin Martia, and Hamid Marvi

***Abstract*—The development, building, and testing of robotic vehicles for applications in deformable media can be costly. Typical approaches rely on full-sized builds empirically evaluating performance metrics such as drawbar pull and slip. Recently developed granular scaling laws offer a new opportunity for terramechanics as a field. Using non-dimensional analysis on the wheel characteristics and treating the terrain as a deformable continuum, the performance of a larger, more massive wheel may be predicted from a smaller one. This allows for new wheel design approaches. However, robot-soil interaction and specific characteristics of the soil or robot dynamics may create discrepancies in prediction. In particular, we find that for a lightweight rover (2–5 kg), the scaling laws significantly overpredicted mechanical power requirements. To further explore the limitations of the current granular scaling laws, a pair of differently sized grousered wheels were tested at three masses and a pair of differently sized sandpaper wheels were tested at two masses across five speeds. Analysis indicates similar error for both designs, a mass dependency for all five pairs that explains the laws' overprediction, and a speed dependency for both of the heaviest sets. The findings create insights for using the laws with lightweight robots in granular media and generalizing granular scaling laws.**

***Index Terms*—Field robots, mining robotics, space robotics and automation, wheeled robots.**

I. Background

ROBOTS traverse granular media through complex motions, often by wheels reacting under primarily normal pressures. Understanding mobility in granular environments is an interest of the robotics, terramechanics, and physics communities [1]–[11]. There are various characteristics such as particle size, size distribution, angularity, material composition, and homogeneity of mixture which can limit the utility of empirical laws or require additional complimentary tests for fitting parameters.

Recent efforts on understanding granular dynamics and craft motion from a more theoretical point of view have produced new models. Granular resistive force theory (RFT) utilizes superposition and discretization of intruders into smaller geometries to sum the resultant forces for analysis [12]–[16]. Theories revolving around granular media as a continuum is another approach with various assumptions about grain bed uniformity utilized in an attempt to model millions of grains as one Coulomb-obedient block [9], [17], [18].

From these efforts, granular scaling laws (GSL) were recently developed [19]. By direct scaling of various parameters such as size and mass, certain outputs such as velocity and power for larger wheels of the same general shape can be predicted from smaller ones. One advantage of exploiting these non-dimensional parameters is the ability to extrapolate performance of field craft in the same granular environment from smaller versions to larger ones, giving greater flexibility to initial testing of designs. These laws include both a gravity variant and invariant version, and hold great potential for the development of field and space robotics.

In this study, we examine the granular scaling laws for boundary case of lightweight robotics. These are often used in practice for space robotics and in labs for prototype and development. Sojourner [20], the Mars rover, is an example of such a class of robot at approximately 11 kg. Prayan, the rover from the Chandrayaan-2 mission [21], is 27 kg. With 6 wheels each, the per-wheel mass weight would be 1.8 kg and 4.5 kg, respectively. Other rovers around this class are the 10 kg Moonraker design [22]. PUFFER [23], [24] is a sub 1 kg rover design and reconfigurable or multi-robot schemes often include light rovers [25]. Some potential use cases on Earth are laboratory developments of new grouser approaches [26], angled granular mobility [27], or other field robotics applications [28]. Whether for space or field robotics, there is a need to understand how lightweight prototypes or rovers may deviate from established granular scaling laws.

II. Granular Scaling Laws (GSL)

This study examines the performance of a lightweight rover equipped with sandpaper wheels for direct comparison to established scaling experiments and grousered wheels to include evaluation of a commonly utilized shape. Wheel grousers are a typical feature for field rovers and to our knowledge, have not been tested for these scaling laws. The grouser design in this study was driven by equations discussed further in this section. We turn first to the dimensions of length, mass, and time which define the wheel and the experiment. The basis of the wheel

Manuscript received September 10, 2019; accepted December 31, 2019. Date of publication January 22, 2020; date of current version January 31, 2020. This letter was recommended for publication by Associate Editor S. Rathinam and Editor D. Song upon evaluation of the reviewers' comments. This work was supported by the Arizona State University. *(Corresponding author: Hamidreza Marvi.)*

The authors are with the School for Engineering of Matter, Transport, and Energy, Ira A. Fulton Schools of Engineering, Arizona State University Tempe, AZ 85287, USA (e-mail: andrew.thoesen@gmail.com; mcbryan.teresa@gmail.com; mkgreencccc@gmail.com; dpmick@asu.edu; jmartia@asu.edu; hmarvi@asu.edu).

This letter has supplementary downloadable material available at https://ieeexplore.ieee.org, provided by the authors.

Digital Object Identifier 10.1109/LRA.2020.2968031

shape was an ABS cylinder covered in either 80-grit sandpaper or printed grousers.

The sizing of the two sets is driven by GSL and we will now briefly expand the explanation of the scaling laws in the literature [19]. First, we have the functional expression followed by a brief description of the physical occurrences:

$$(P, V) = \psi(d, l, m, \omega, t, f, g, \rho, \mu, \mu_w) \tag{1}$$

We are interested in power P and translational velocity V. These occur as a function of the wheel and its interaction with the environment. The wheel is described by its characteristic length (typically radius) l, its thickness (depth into the page) d, its mass m, a driving rotational velocity ω, and a consistent shape outline f. This shape outline f is a dimensionless set of points which sets the condition that although the wheel shape may be arbitrary, it must be consistent when scaling. We cannot, for example, scale grousered wheel results for a sandpaper wheel. The environment is described by gravity g and the granular characteristics ρ, μ, and μ_w which are the density, internal granular friction, and wheel-grain friction. The system is dependent on time, t. By using non-dimensional analysis and a careful set of assumptions discussed in the referenced paper, the result is as follows [19]:

$$\left[\frac{P}{Mg\sqrt{Lg}}, \frac{V}{\sqrt{Lg}}\right] = \Psi\left(\sqrt{\frac{g}{L}}t, f, \frac{g}{L\omega^2}, \frac{DL^2}{M}\right) \tag{2}$$

For the purposes of this paper, we will utilize the gravity-invariant laws that are as follows:

$$\left[\frac{P}{M\sqrt{L}}, \frac{V}{\sqrt{L}}\right] = \tilde{\Psi}\left(\sqrt{\frac{1}{L}}t, f, \frac{1}{L\omega^2}, \frac{DL^2}{M}\right) \tag{3}$$

The above equation shows the functional relationship of the parameters to be scaled. If a wheel with the inputs of (L, M, D, ω) is compared to a wheel affected by positive scalars r and s, the predicted relationship $(L,' M,' D,' \omega') = (rL, sM, \frac{s}{r^2}D, \frac{1}{\sqrt{r}}\omega)$ follows. The conclusion is that one should be able to predict the time-averaged power and translational velocity of a rotating wheel with the following relationship:

$$P' = s\sqrt{r}P \tag{4}$$

$$V' = \sqrt{r}V \tag{5}$$

III. Experimental Design

The experiments in this study were designed to replicate verified experimental conditions for GSL except for the control variables of interest. One such variable is changing the wheel shape to that of a grousered wheel. One recalls that in Eq.(3), f is the symbolic representation that the depth-invariant shape of the wheel is consistent through any dimensional changes. The shape of a straight grousered wheel adheres to this assumption for the scaling laws. Previous research indicates that the mobility gains of grousered wheels compared to smooth in soils are most likely due to a change in soil motion, not an increase in thrust [29], [30]. The root cause of this is the "pre-clearing" of granular material in front of the leading wheel edge before it makes contact, thus lowering the contact angle and compaction/motion resistance of the media, rather than addition of thrust from the paddle-like shape as one might infer. Thus, while the outline of a grousered wheel obeys GSL, and the flow characteristics may scale, the complexities of granular motion to the grousers mean an examination of GSL for this application is necessary.

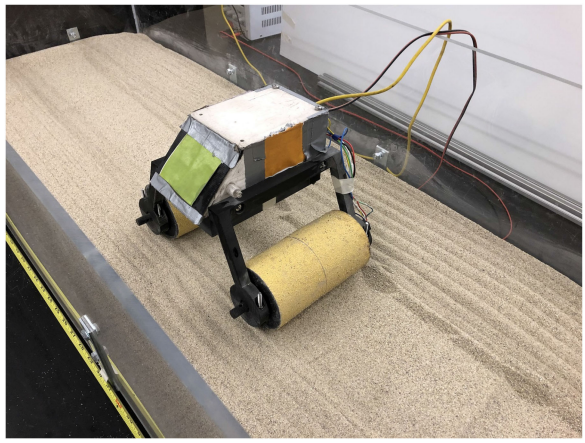

Fig. 1. Craft with small sandpaper wheels.

The minimum number of grousers necessary to achieve such "pre-clearing" was determined by an equation from the literature [31] with the conservative assumption of 20% slip and approximately 2 cm of sinkage; neither of which appeared reached during experiments. The set of grouser parameters, along with the wheel characteristics, are shown in Table I. The minimum number of grousers required to clear material from the contact edge can be calculated according to the following inequality [31]:

$$\Phi < \frac{1}{1-i}\left(\sqrt{(1+h)^2 - (1-z)^2} - \sqrt{1-(1-z)^2}\right), \tag{6}$$

where Φ is the spacing required between the grousers in radians, i is estimated slip, h is grouser height, and z is estimated sinkage. To ensure the next grouser encounters soil before the wheel rim does, the placement of grousers around the wheel must be Φ radians or less. In keeping with GSL, we maintained the number of grousers between designs when enlarging the shape. The minimum for the smaller wheels was 14 grousers, which also exceeded the necessary number of 13 for larger wheels. The craft was designed to be multi-purpose, allowing wheels to be easily interchanged with other wheel designs. A modular undercarriage weight holder was added to the bottom of the craft. Feet height were designed to keep center of gravity as low as possible without interfering with the granular flow. Craft and sand bed for experiments are featured in Fig. 1.

The general dimensions and experimental parameters for these wheels are found in Table I. These classically grousered wheels (GSL1G and GSL2G) use the same wheel sizing as the sandpaper wheels. The sandpaper wheels (GSL1SP and GSL2SP) have an identical body print to the grousered wheels but have 80-grit sandpaper adhered around the entire surface. The two types of wheels are shown in Fig. 2. For purposes of simplification, the thickness of the wheel is kept constant between the two sets. The mass and diameter of the wheels were varied according to scaling laws, as were the target RPM's.

TABLE I
PROPERTIES OF GROUSER AND SANDPAPER WHEEL SETS TESTED

Name	Diameter (cm)	Masses (kg)	Thickness (cm)	Grouser Length (cm)	ω (RPM)
GSL1G	7.5	1.46, 2.19, 2.92	14	1.25	15,30,45,60,75
GSL2G	10	2.59, 3.84, 5.19	14	1.667	13,26,39,52,65
GSL1SP	7.5	1.46, 2.92	14	N/A	15,30,45,60,75
GSL2SP	10	2.59, 5.19	14	N/A	13,26,39,52,65

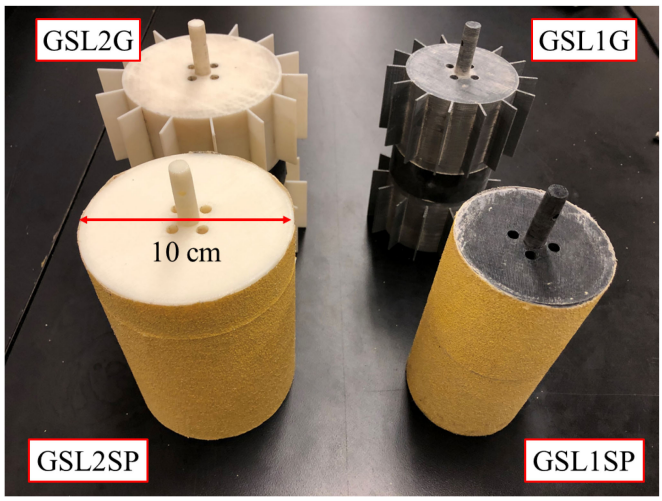

Fig. 2. The wheels used in this study labelled with their designations. Grousered wheels of both sizes are seen in the back and sandpaper wheels of both sizes are seen in the front.

For the experiments themselves, we make several assumptions:

1) We assume granular motion in the direction perpendicular to travel, i.e. out of plane is minimal.
2) We assume consistent media; the results of a smaller robot in one granular media should not be used to predict large robot performance in a different media. The relevant granular properties were decomposed into the dimensionless friction coefficient of wheel-sand interaction, the internal friction, and the expression for density. Assuming all three are consistent in the media, we eliminate the frictions and remove ρ from our equations.
3) We assume constant gravity, and use the gravity-invariant laws.

The experiments were performed in the sand bed shown in Fig. 1. The bed itself is an acrylic box of 2 meters long and 40 cm wide with 10 cm depth of sand. The sand is Quikrete medium, a well-characterized construction sand. The craft is driven by a wired power supply. This feeds into a motor driver, which distributes the load through a current sensor to each 12 V motor. This process is controlled by an Arduino Uno microcontroller board and the data of the motor encoders and the current sensors are fed back to this microcontroller.

The mass was adjusted to the required amount for each wheel set. The craft was placed at one end of the box, set to run at a specified target speed, and allowed to travel from one end to another. After each trial, the sand was tilled with a thatch rake in the direction of travel to prepare the sand consistently for each experiment. Ten trials were performed for each set of wheels at each of the five different rotational speeds. All hardware was consistent between trials aside from the wheels and the added mass.

The no-load current of each individual motor was measured with benchtop testing. This current was subtracted from the measured motor load to estimate the torque value from the current-torque relationship of the motor during runs. This relationship is a function of the physical design of the motor and was provided by the manufacturer. By using this torque estimation and the measured rotational speed, the mechanical power of each set was estimated.

Examining the test parameters in Table I for both wheel shapes, we see that the large set diameter is scaled by 1.333 compared to the smaller set. The large set mass is scaled by the square of this, 1.778, compared to the mass of the smaller sets. This leads to identical thickness in the smaller and larger wheels and means according to Eq.(5), the predicted power of the GSL2 sets should always be at a ratio of 2.05 to that of GSL1. If this holds true, the scaling laws are accurate for lightweight wheeled rovers in granular media. These evaluations also require that the larger sets occur at specific speeds. Using a PID controller, we ensured speeds were very close to those targeted (within 3% error). Upon observing a linear relationship between the mechanical power and speed, we used a linear regression and the target speed to estimate the power at the exact speed the scaling laws required for comparison.

IV. RESULTS AND DISCUSSION

A. *Mass/Pressure Dependence of Wheeled Granular Scaling Laws*

The study was designed to evaluate whether the scaling laws could apply to a lightweight robot and what deviations might be found. A light, medium, and heavy set of masses for grousered wheels and a light and heavy set of masses for sandpaper wheels were run (see Table I for details). With these masses and the two wheel sizes, the target power ratio for all sets was 2.05 by design. The power ratio is the ratio of required mechanical power in the larger wheel to the power in the smaller wheel for a wheel pair, i.e. all larger craft results should require double the mechanical power of their smaller counterparts. This power ratio emerged as a balance between creating a discernible difference in large and small wheel power draw and avoiding the limits of the motor performance. It also fits within the limits of the environment, the maximum size of printed wheel, and the power transfer system from motor to wheel. Each one of these was evaluated at five speeds. The full details are listed in Table I, and the larger craft mass was used for comparison in both Fig. 3 and Fig. 4.

TABLE II
POWER RATIOS AND ERRORS FOR ALL SPEEDS

Target RPM	GSL12SP Light	Error	GSL12SP Medium	Error	GSL12SP Heavy	Error
13	1.59	22.6%	-	-	1.98	3.6%
26	1.47	28.1%	-	-	1.85	9.6%
39	1.38	32.8%	-	-	1.83	10.9%
52	1.55	24.2%	-	-	1.75	14.5%
65	1.49	27.3%	-	-	1.69	17.3%
Target RPM	**GSL12G Light**	**Error**	**GSL12G Medium**	**Error**	**GSL12G Heavy**	**Total Error**
13	1.48	27.7%	1.70	17.2%	N/A*	N/A*
26	1.64	20.1%	1.66	19.0%	1.84	10.3%
39	1.59	22.4%	1.70	17.1%	1.80	12.4%
52	1.54	25.0%	1.65	19.5%	1.77	13.5%
65	1.59	22.3%	1.66	18.8%	N/A*	N/A*

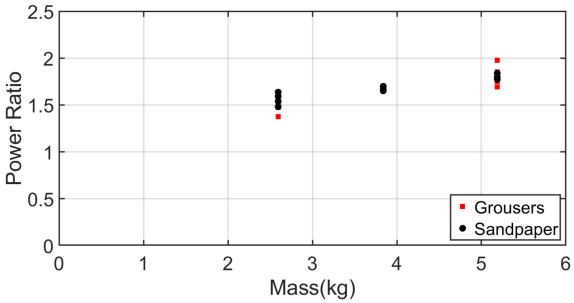

Fig. 3. The relationship between mass and power ratio (large set mechanical power over smaller set mechanical power) for both types of wheels.

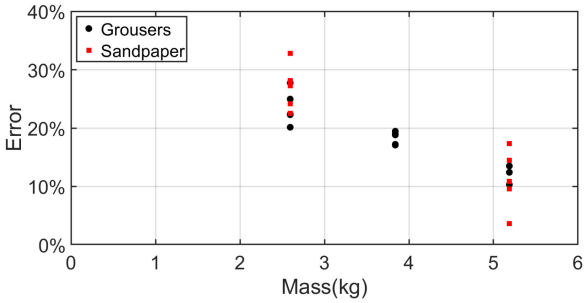

Fig. 4. The error percentage as a function of mass. The error percentage is defined as the difference between the experimental power ratio and the target of 2.05, over 2.05.

In the study by Slonaker *et al.*, the original tests were run with masses between 13.4 kg and 45.7 kg for all sets [19]. In those tests, all sets reportedly followed their scaling predictions within an error of 3%. Those experiments were run with a single wheel on a gantry with the direction of travel constrained in a planar fashion. They were also run with all sets below 30 RPM. Here, the lowest mass is 1.46 kg and the largest is 5.19 kg. The total mechanical power comes from two wheels, and the craft is not constrained to move in a planar fashion although it generally did so as seen in the supplemental video. This mobility was allowed to evaluate more field-like conditions. The target speeds range from 15–75 RPM for smaller wheels and 13–65 RPM for larger ones. This different set of lighter, faster parameters was targeted to explore a design space closer to that of laboratory robots and small prototypes rather than fully sized vehicles.

The target power ratio of 2.05 was not reached for any of the experiments (Fig. 3). Instead, a mass-dependency was noted in the power ratio and error percentage rather than a consistent ratio of 2.05 as predicted. The raw values for all 25 combinations of masses-speeds are shown in Table II with both power ratio and error listed. Interestingly, the closest case to target value was the heaviest sandpaper wheel set at the lowest speed; this particular condition was the closest to the experiments performed by Slonaker *et al.* [19].

An alternative expression of the power ratio data is shown in Fig. 4 as an error percentage versus mass. The error percentage is defined as the difference between the experimental power ratio and the target of 2.05, over 2.05. A linear regression approximated the heaviest mass would need to be at 8 kg to attenuate the error to zero.

On this note, we now give our hypothesis for why the error is high when the observed physics appear similar to the case reported in [19]. To investigate the root cause of the error, a total of 40 trials with raked sand were performed during secondary tests to further investigate the source of error. This was done with both wheel shapes, at the largest and smallest masses, using the larger GSL2 sizing for each shape, and at the lowest speeds to control for the observed inertial errors. Each set was performed at ten trials apiece. A sliding rigid bar used with an attached caliper to measure the difference between the peaks and valleys of the raking pattern. An average difference for all 40 trials of 1.58 $\pm$ 0.18 mm was found. The raked case for sandpaper wheels, with measurements made from the high point of the raked sand, showed sinkage of 2.69 $\pm$ 0.29 mm and 2.82 $\pm$ 0.18 mm for light and heavy cases. The grousered wheels showed 2.02 $\pm$ 0.19 mm and 2.51 $\pm$ 0.28 mm for light and heavy cases, respectively.

In sum, since the depth of the raking pattern on the surface is of comparable magnitude to the sinkage, we conclude that this likely contributed to the scaling deviations. In particular, as a result of raking the grain packing fraction was altered within the range of sinkages observed. This may have changed the effective friction of the granular media to a degree that violated the assumption of the environment having a consistent friction coefficient.

Secondary experiments to investigate the error were performed to measure the depth of sinkage using pre- and post-run caliper measurements. All experiments were performed

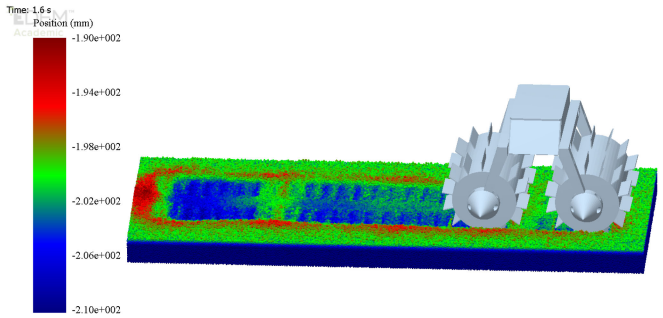

Fig. 5. Simulation of a grousered rover traversing granular media at 52 RPM. Cooler colors indicate deeper impressions.

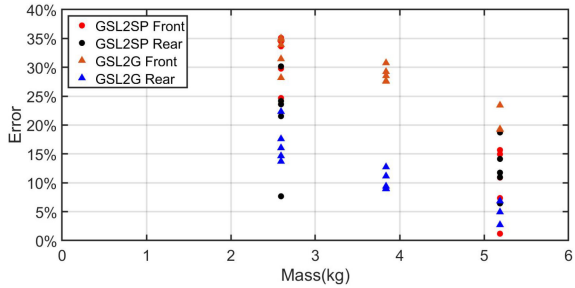

Fig. 6. Error of each dataset for individual motor power; the front motors have significantly more error than rear motors.

at 16 RPM to mitigate inertial effects. The caliper measurements for unraked, level sand trials show minimal sinkage. The smallest and biggest masses on GSL2 sandpaper wheels had 1.00 ± 0.24 mm and 1.09 ± 0.24 mm sinkage, respectively, while the grousered wheels had 0.69 ± 0.12 mm and 0.92 ± 0.12 mm for light and heavy GSL2G wheels. Given that the particle size of the Quikrete sand is generally between 300-800 microns, a depth of ten grain diameters would be between 3-8 mm. Neither the level sand sinkage nor the raked sand sinkage was observed to exceed 3 mm on average for these tests.

We conclude that the shallow wheel sinkage, on the order of 10 grain diameters or smaller, may have been subjected to grain-size effects that caused the sand response to deviate from the frictional plasticity which underpins the scaling theory. In particular, shallow sinkage alone and/or combined with a characteristic raking pattern of close magnitude is the probable cause of scaling error. This notably explains the apparent dependence on mass. Thus, it is recommended that a minimal baseline test of sinkage depth is performed first before using the granular scaling laws for smaller massed craft, although the response will depend on multiple factors such as granular media, wheel shape, and size.

B. Preliminary Discrete Element Method Simulations

An additional insight into the experimental error was gained from preliminary Discrete Element Method (DEM) simulations. DEM simulations model individual particles to simulate granular flow and when coupled with multi-body dynamics (MBD), vehicle dynamics across deformable terrain may be evaluated. Using identical masses and sizes for GSL1G and GSL2G light pair, simulations were performed at 30 RPM and 60 RPM for GSL1G and 26 RPM and 52 RPM at GSL2G (Fig. 5) in accordance with scaling law factors. The scaling laws found predictions within 6.5% of DEM simulation results at the same light masses which showed 25% error in experiments (Fig. 5). Major differences include lowering the Young's modulus of the grains and a grain size increase to decrease the computational cost without significantly sacrificing the macro scale interactions [2]–[4]. These simulations were run with silica sand properties [32]. Notably, the surface in simulation is perfectly level to the vertical axis of gravity, compared to minor inconsistencies which can occur in real world experimentation. It was also unraked, compared to the original experiments, which has been discussed as a source of error. The more strictly controlled environment, combined with an absence of raking pattern depths which are as large as the sinkage, is the most likely explanation for DEM success of scaling laws but experimental error.

C. Leading and Lagging Motor Error Difference

The final observation on mass-error dependency is the difference observed between leading and lagging motors in the grousered wheels as seen in Fig. 6. If the two wheels are treated independently and the power ratios of the leading/lagging wheels are evaluated, some additional salient trends emerge. Notably, although the sandpaper wheels did not show high differentiation in error between leading and lagging wheels, the grousered wheels showed significant difference with the rear wheels drawing higher power ratio and lower errors in all cases. Our hypothesis is that since robot dynamics shifts weight towards the back, the ability of grousers to pre-clear sand and reduce sinkage was partly mitigated. This would press the back wheels further into the sand. Additionally, although the wheel difference is less pronounced in the sandpaper wheels, it is still present. The effect in both could be explained by the pre-compaction of the sand by the first wheel before the second wheel rolls over it. This would partly counteract the lack of uniformity in friction coefficient caused by packing fraction issues from raking and low sinkage, and therefore would lower the scaling discrepancies.

D. Velocity/Inertia Dependence of Wheeled Granular Scaling Laws

We turn now to the velocity dependence of the power ratios. In figure Fig. 7, power ratios are graphed versus wheel rotational speed. For all sets, there is a weak function of power ratio versus speed with slope of -0.0014 power ratio/RPM. The power ratio decreases minimally with increased velocity for the experiments in general. In addition, the heaviest sets show the highest dependence on velocity; linear regression shows almost double and quadruple the slopes compared to the group as a whole for grousered wheels with slope of -0.026 and sandpaper wheels with slope of -0.0052, respectively. For context, the

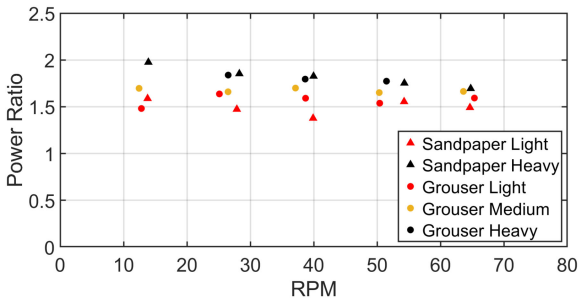

Fig. 7. Power ratio versus wheel RPM. Power ratio trend of all data points shows a decrease with wheel rotational speed. Furthermore, power ratios of heaviest data points show significantly more decline with speed than lighter sets.

original scaling law experiments presented in [19] had speeds between 14–28.6 RPM and no relationship between power ratio and velocity at different masses was observed. This is a limitation that one must bear in mind for using these laws to approximate robot power draw at higher speeds for light-weight rovers. It is possible that this scaling error as a function of wheel rotation velocity is reduced or disappears at higher masses.

V. Conclusion and Future Directions

Through a series of 500 trials, we have evaluated the accuracy of predicting mechanical power draw using granular scaling laws for lightweight rovers. The results indicate inconsistency with the laws at the masses (1.5–5.2 kg) and speeds (13–75 RPM) tested, although the heaviest and slowest sandpaper case showed 3.6% error, within reported literature accuracy. The results of this inaccuracy can be seen as a strong function of the mass, likely due to lightweight rovers creating subcritical amounts of sinkage to fully engage the soil at a level which is necessary for scaling to be accurate. The results can also be seen as a weak function of rotational wheel speed, likely due to inertial effects. The results show lower error for grousered wheels than sandpaper at the light masses but this difference is eliminated at the heavy masses. Furthermore, there is lower error for lagging wheels than leading wheels in the grousered sets, likely because of vehicle dynamics and more effective lead wheel grouser clearing. However, the results do not indicate significant deviation due to grouser inclusion; it is possible that grousered wheels on a vehicle of sufficient mass will follow predictions.

For future directions, there are several variables which could be controlled and evaluated. A study ranging across 2.6 kg (the smallest mass used in our larger wheel tests) to 29.3 kg (the smallest mass used by Slonaker *et al.* in their larger wheel sizes) in a well characterized sand could fully evaluate the relationship between mass (or pressure/sinkage) and scaling error. Direct measurement of sinkage or pressure in this case would provide the most straightforward answer. One possible avenue for this would also be further coupled Multi-body Dynamics (MBD) and DEM simulations to evaluate the scaling laws considering gravity variance as well. DEM simulations of related experiments using a different granular material and wheel design show promise for scaling predictions of light craft but more investigation is needed.

Acknowledgment

The authors would like to thank members of the BIRTH Lab for their assistance and Arizona State University for funding.

References

[1] H. Marvi *et al.*, "Sidewinding with minimal slip: Snake and robot ascent of sandy slopes," *Science*, vol. 346, no. 6206, pp. 224–229, 2014.
[2] A. Thoesen, S. Ramirez, and H. Marvi, "Screw-generated forces in granular media: Experimental, computational, and analytical comparison," *AIChE J.*, vol. 65, no. 3, pp. 894–903, 2019.
[3] A. Thoesen, T. McBryan, and H. Marvi, "Helically-driven granular mobility and gravity-variant scaling relations," *RSC Adv.*, vol. 9, no. 22, pp. 12 572–12 579, 2019.
[4] A. Thoesen, S. Ramirez, and H. Marvi, "Screw-powered propulsion in granular media: An experimental and computational study," in *Proc. IEEE Int. Conf. Robot. Autom.*, 2018, pp. 1–6.
[5] M. Grujicic, H. Marvi, G. Arakere, W. Bell, and I. Haque, "The effect of up-armoring of the high-mobility multi-purpose wheeled vehicle (HMMWV) on the off-road vehicle performance," *Multidiscipline Model. Mater. Structures*, vol. 6, no. 2, pp. 229–256, 2010.
[6] M. Grujicic, H. Marvi, G. Arakere, and I. Haque, "A finite element analysis of pneumatic-tire/sand interactions during off-road vehicle travel," *Multidiscipline Model. Mater. Structures*, vol. 6, no. 2, pp. 284–308, 2010.
[7] H. Bagheri, V. Taduru, S. Panchal, S. White, and H. Marvi, "Animal and robotic locomotion on wet granular media," in *Proc. Conf. Biomimetic Biohybrid Syst.*, 2017, pp. 13–24.
[8] S. Kamath, A. Kunte, P. Doshi, and A. V. Orpe, "Flow of granular matter in a silo with multiple exit orifices: Jamming to mixing," *Physical Rev. E*, vol. 90, no. 6, 2014, Art. no. 062206.
[9] K. Kamrin, "Nonlinear elasto-plastic model for dense granular flow," *Int. J. Plasticity*, vol. 26, no. 2, pp. 167–188, 2010.
[10] S. Lee and D. B. Marghitu, "Multiple impacts of a planar kinematic chain with a granular matter," *Int. J. Mech. Sci.*, vol. 51, no. 11/12, pp. 881–887, 2009.
[11] H. Omori, T. Murakami, H. Nagai, T. Nakamura, and T. Kubota, "Validation of the measuring condition for a planetary subsurface explorer robot that uses peristaltic crawling," in *Proc. IEEE Aerosp. Conf.*, 2013, pp. 1–9.
[12] R. D. Maladen, Y. Ding, P. B. Umbanhowar, A. Kamor, and D. I. Goldman, "Mechanical models of sandfish locomotion reveal principles of high performance subsurface sand-swimming," *J. Royal Soc. Interface*, vol. 8, no. 62, pp. 1332–1345, 2011.
[13] Y. Ding, S. S. Sharpe, A. Masse, and D. I. Goldman, "Mechanics of undulatory swimming in a frictional fluid," *PLoS Comput. Biol.*, vol. 8, no. 12, 2012 , Art. no. e1002810.
[14] C. Li, T. Zhang, and D. I. Goldman, "A terradynamics of legged locomotion on granular media," *Science*, vol. 339, no. 6126, pp. 1408–1412, 2013.
[15] T. Zhang and D. I. Goldman, "The effectiveness of resistive force theory in granular locomotion," *Phys. Fluids*, vol. 26, no. 10, 2014, Art. no. 101308.
[16] Y. O. Aydin *et al.*, "Geometric mechanics applied to tetrapod locomotion on granular media," in *Proc. Conf. Biomimetic Biohybrid Syst.*, 2017, pp. 595–603.
[17] S. Dunatunga and K. Kamrin, "Continuum modelling and simulation of granular flows through their many phases," *J. Fluid Mechanics*, vol. 779, pp. 483–513, 2015.
[18] S. Dunatunga and K. Kamrin, "Continuum modeling of projectile impact and penetration in dry granular media," *J. Mechanics Phys. Solids*, vol. 100, pp. 45–60, 2017.
[19] J. Slonaker *et al.*, "General scaling relations for locomotion in granular media," *Physical Rev. E*, vol. 95, no. 5, 2017, Art. no. 052901.
[20] R. Team, "Characterization of the martian surface deposits by the mars pathfinder rover, sojourner," *Science*, vol. 278, no. 5344, pp. 1765–1768, 1997.
[21] J. N. Goswami and M. Annadurai, "Chandrayaan-2 mission," in *Proc. Lunar Planetary Sci. Conf.*, vol. 42, 2011, Art no.. 2042.
[22] K. Yoshida, N. Britton, and J. Walker, "Development and field testing of moonraker: a four-wheel rover in minimal design," in *Proc. 12th Int. Symp. Artif. Intell., Robot. Automat. Space*, 2013.

[23] J. T. Karras, C. Fuller, K. C. Carpenter, A. Buscicchio, and C. E. Parcheta, "Puffer: pop-up flat folding explorer robot," U. S. Patent App. 15/272,239, Mar. 30 2017.
[24] J. T. Karras *et al.*, "Pop-up mars rover with textile-enhanced rigid-flex PCB body," in *Proc. IEEE Int. Conf. Robot. Autom.*, 2017, pp. 5459–5466.
[25] T. M. Roehr, F. Cordes, and F. Kirchner, "Reconfigurable integrated multirobot exploration system (RIMRES): Heterogeneous modular reconfigurable robots for space exploration," *J. Field Robot.*, vol. 31, no. 1, pp. 3–34, 2014.
[26] A. N. Ibrahim, S. Aoshima, and Y. Fukuoka, "Development of wheeled rover for traversing steep slope of cohesionless sand with stuck recovery using assistive grousers," in *Proc. IEEE Int. Conf. Robot. Biomimetics (ROBIO)*, 2016, pp. 1570–1575.
[27] H. Inotsume, M. Sutoh, K. Nagaoka, K. Nagatani, and K. Yoshida, "Modeling, analysis, and control of an actively reconfigurable planetary rover for traversing slopes covered with loose soil," *J. Field Robot.*, vol. 30, no. 6, pp. 875–896, 2013.
[28] Y. Yamada, Y. Miyagawa, R. Yokoto, and G. Endo, "Development of a blade-type crawler mechanism for a fast deployment task to observe eruptions on Mt. mihara," *J. Field Robot.*, vol. 33, no. 3, pp. 371–390, 2016.
[29] S. Moreland, K. Skonieczny, H. Inotsume, and D. Wettergreen, "Soil behavior of wheels with grousers for planetary rovers," in *Proc. IEEE Aerosp. Conf.*, 2012, pp. 1–8.
[30] S. J. Moreland, "Traction processes of wheels on loose, granular soil," Ph.D. dissertation, Doctoral Dissertation, Carnegie Mellon Univ., Pittsburgh, PA, United States, 2013.
[31] K. Skonieczny, S. J. Moreland, and D. S. Wettergreen, "A grouser spacing equation for determining appropriate geometry of planetary rover wheels," in *Proc. IEEE/RSJ Int. Conf. Intell. Robots Syst.*, 2012, pp. 5065–5070.
[32] M. Cil and K. Alshibli, "3D assessment of fracture of sand particles using discrete element method," *Géotechnique Lett.*, vol. 2, no. 3, pp. 161–166, 2012.